HHS Public Access

Author manuscript

Cancer Res. Author manuscript; available in PMC 2017 February 01.

Published in final edited form as:

Cancer Res. 2016 February 1; 76(3): 630–642. doi:10.1158/0008-5472.CAN-15-0940.

Systemic Chromosome Instability (CIN) resulted in colonic transcriptomic changes in metabolic, proliferation, and stem cell regulators in Sgo1-/+ mice

Chinthalapally V. Rao[1], **Saira Sanghera**[2], **Yuting Zhang**[1], **Laura Biddick**[1], **Arun Reddy**[1], **Stan Lightfoot**[1], **Naveena B. Janakiram**[1], **Altaf Mohammed**[1], **Wei Dai**[3], and **Hiroshi Y. Yamada**[1]

[1]Center for Cancer Prevention and Drug Development, Department of Medicine, Hematology/Oncology Section, University of Oklahoma Health Sciences Center (OUHSC), Oklahoma City, OK

[2]College of Arts & Sciences, Baylor University, Waco, TX

[3]Department of Environmental Medicine, New York University Langone Medical Center, Tuxedo, NY

Abstract

Colon cancer is the second most lethal cancer and is predicted to claim 49,700 lives in the U.S this year. Chromosome Instability (CIN) is observed in 80–90% of colon cancers and is thought to contribute to colon cancer progression and recurrence. To investigate the impact of CIN on colon cancer development, we developed shugoshin-1 (Sgo1) haploinsufficient (-/+) mice, an animal model focusing on mitotic error-induced CIN. In this study, we analyzed signature changes in the colonic transcriptome of Sgo1-/+ mice to examine the molecular events underlying the altered carcinogenesis profiles in Sgo1-/+ mice. We performed next-generation sequencing of normal-looking colonic mucosal tissue from mice treated with the carcinogen azoxymethane (AOM) after 24 weeks. Transcriptome profiling revealed 349 hits with a 2-fold expression difference threshold (217 upregulated genes, 132 downregulated genes, p=0.05). Pathway analyses indicated that the Sgo1-CIN-tissues upregulatedpathways known to be activated in colon cancer, including lipid metabolism (Z score 4.47), Notch signaling (4.47), insulin signaling (3.81), and peroxisome proliferator-activated receptor (PPAR) pathways (3.75), and downregulated pathways involved in immune responses including allograft rejection (6.69) and graft-versus-host disease (6.54). Notably, stem cell markers were also misregulated. Collectively, our findings demonstrate that systemic CIN results in transcriptomic changes in metabolism, proliferation, cell fate, and immune responses in the colon, which may foster a microenvironment amenable to cancer development. Therefore, therapeutic approaches focusing on these identified pathways may be valuable for colon cancer prevention and treatment.

Correspond with: Hiroshi Y. Yamada (Hiroshi-yamada@ouhsc.edu) Phone 405-227-8001 x32524 Fax 405-271-3225, Department of Medicine, Hem/Onc Section, University of Oklahoma Health Sciences Center (OUHSC), 975 NE 10th St. BRC1207, Oklahoma City, Oklahoma 73104.

Conflict of interest

The authors declare no conflicts of interest.

Keywords

Shugoshin 1(Sgo1); Chromosome Instability (CIN); mice; colon; transcriptome

Introduction

Chromosome instability (CIN) is primarily caused by impaired mitotic fidelity, and leads to aneuploidy (1). CIN and aneuploidy are hallmarks of numerous cancers. In addition, CIN is especially prevalent in colon cancer (80–90%) and is associated with poor prognosis (2). A study in Mad2-CIN mice model even suggested that CIN is causal to higher cancer recurrence (3). The remaining 10–20% of cases are associated with microsatellite instability (MIN), which is primarily caused by defects in DNA metabolism, especially in mismatch repair pathways (4). As colon cancer is the second most lethal cancer and is predicted to claim 49,700 lives this year in the U.S. alone (5), investigating CIN has high clinical relevance. The high prevalence of CIN among colon cancer may be due to CIN-causing mutations' involvement in colonic carcinogenesis itself. Many gene mutations that occur frequently in colon cancer, such as mutations in TP53, APC, and FBXW7 (6), can cause CIN, suggesting a strong link between the initiation and progression of colonic carcinogenesis and CIN (7). Researchers have attempted to use various model systems, including *Drosophila* (8), yeast (9), and aneuploid mice (10), to characterize CIN and aneuploidy, in hopes of elucidating the relationship between CIN and carcinogenesis and of developing a CIN/aneuploidy-targeting approach for cancer prevention or therapy (11–14). Models of CIN, including BubR1$^{-/+}$, Mad2$^{-/+}$, and cenpe$^{-/+}$ mice, demonstrated organ-specific oncogenic and tumor-suppressing effects (15. 16).

We developed a mouse model of CIN, the haploinsufficient (-/+) Shugoshin 1 (Sgo1) mouse. Approximately 48% of human colon cancers expressed less than 50% of Sgo1 mRNA (17), and 13% expressed abnormal dominant-negative Sgo1 transcript (18), suggesting a role of Sgo1 in human colon cancer. Sgo1 protein plays dual roles in cells as a centrosome component and as an accessory factor for the cohesin-mediated tethering of mitotic chromosomes. Sgo1 insufficiency resulted in reduced Sgo1 protein and partial loss of function. Consistently, Sgo1$^{-/+}$ fibroblasts showed an increase in multiple centrosomes and mitotic abnormalities, for example, premature chromosome separation and lagging chromosomes, that led to CIN (19), supporting the notion that the Sgo1 model would be valid for investigating the CIN-carcinogenesis relationship in select organs.

From the cancer profile, we hypothesized that the Sgo1 mouse may also provide a valid study model for lung and liver cancers, in addition to colon cancer. The mitotic process and the centrosome are both also targeted by hepatitis viruses like HBV and HCV (20–24). We have recently shown that the Sgo1 mouse as a possible model for viral liver cancer. Liver tissues from Sgo1$^{-/+}$ mice showed an increase in hepatocytes with multiple centrosomes (25). After treatment with colonic and hepatic carcinogen azoxymethane (AOM), Sgo1$^{-/+}$ mice showed rapid development of precancerous aberrant crypt foci (ACF) [$p<0.05$; (19)] and hepatocarcinoma [$p<0.05$; (25)], indicating that CIN can aggravate colonic and hepatic carcinogenesis.

From the previous result in colon (19), we anticipated that with AOM treatments Sgo1 would develop later stage colon tumors straightforwardly. To test the prediction, we performed time course experiment monitoring carcinogenesis in three endpoints (12, 24, 36 weeks) after AOM treatments (26). Consistent with the prediction, Sgo1 mice rapidly developed more ACF due to activation of the oncogenic IL-6 and Bcl-2 pathways. However, unexpectedly, by the 24 weeks endpoint, many of the ACF and microtumors regressed in Sgo1. The result was partially explained by activated tumor suppressors INK4A (p16) and CDKN1A (p21) (26). Thus carcinogenesis seemed to depend on balance among antagonizing pathways, yet the characterization was limited to select markers and was not comprehensive (19, 26). We posited that molecular events that are innate to the high CIN tissue of $Sgo1^{-/+}$ are responsible for the differential dynamics in colonic carcinogenesis, and intended to identify the specific events.

Here, we report colonic transcriptomic signatures in $Sgo1^{-/+}$ mice by comparing the transcriptome in normal-looking colonic mucosal tissues from Sgo1 mice with those from control wild-type mice. Although the use of genetically defined models aids in the identification of key changes without the complications of human tumor heterogeneity, to our knowledge, transcriptome analysis for transgenic CIN models has never been published. The human colon cancer transcriptome has been investigated (e.g. 27, 28), yet characterization of the relationship between high CIN and the cancer transcriptome is limited (29). Our transcriptomic analyses showed unexpected results. Since CIN starts early in colonic carcinogenesis (7), our results will aid in developing the framework for a targeted approach to chemoprevention at a seminal stage of carcinogenesis, and/or to identify markers for risk assessment.

Materials and Methods

Transgenic mice and tissue samples

Details for the generation of Sgo1 haploinsufficient (-/+) mice, the carcinogenesis assay with AOM treatment, and sample collection were described previously (25, 26). Briefly, we bred forty-five female wild-type mice and forty-five female $Sgo1^{-/+}$ mice. All mice were generated with the low-cancer-susceptible C57BL/6 background, and maintained in the OUHSC Biomedical Research Center rodent barrier facility. Standard diet (Purina, MO) was fed throughout the experiment. On the 7^{th} week after birth, the mice were grouped. Beginning in the 8th week, all mice were intraperitoneally injected with 4 mg/kg AOM diluted in 0.9% saline, twice a week for four weeks (8 administrations in total). We euthanized 15 wild-type mice and 15 $Sgo1^{-/+}$ mice using CO_2 asphyxiation at three different time points: the 12^{th}, 24^{th}, and 36^{th} weeks after completion of AOM treatment. At each end point, we performed necropsies with gross examinations for tumors and any abnormalities, and collected normal-looking colonic mucosal tissue by scraping. Visible tumors were collected separately. The scraped colonic mucosal tissues and tumors were snap-frozen in liquid nitrogen, and stored in a −80°C freezer. For ACF and tumor counting, colons were cut open longitudinally and fixed in 10% formalin. ACF were counted using methylene blue staining and bright field microscopy. Once the ACF counting was complete, we embedded the colons in paraffin and made sections with a microtome for immunohistochemistry (IHC).

All treatments were in compliance with protocols approved by the OUHSC institutional animal care and use committee. For CD36 expression analysis, untreated WT, Sgo1 and BubR1 mice were maintained for 12 months, and for *apc* mice, 3.5 months. For immune function analysis, we used 11–12 months old untreated female WT (N=3) and Sgo1 (N=3) mice. Colons were collected and cut longitudinally. A half of colon was used for colonocytes recovery and FACS sorting, and the other half was preserved in OTC in dry ice/methanol bath then −80°C for cryosectioning and immunofluorescence. The authors thank Histology and Immunohistochemistry Core at PC Stephenson Cancer Center, OUHSC for their help with tissue processing and cryosectioning.

Next Generation Sequencing (NGS)/RNA-seq and data analyses

Normal-looking parts of colonic mucosal tissues were scraped from at least six wild-type and six Sgo1 mice, all treated with AOM, at 24 weeks after the completion of AOM treatment. Total RNA was extracted with Trizol reagent (Life Technologies, San Francisco, CA) and subjected to cDNA library construction, followed by NGS per the NGS protocol with an Illumina sequencer in the OUHSC core facility (Microgen) with the aid of Dr. Allison Gillaspy and Dr. Lydgia Jackson. The sequence data was deposited to the Geospiza/Perkin Elmer (Seattle, WA) company server and analyzed with GeneSifter bioinformatics software. The dataset was also deposited to NIH-GEO database (accession number GSE73100).

The same data set was also analyzed with Strand bioinformatics software (Strand-NGS, San Francisco, CA). Illumina MiSeq paired fastq files were aligned in Strand NGS software version 2.1 (www.strand-ngs.com) using mouse mm10 (UCSC) assembly. The Dec. 2011 Mus musculus assembly (Genome Reference Consortium Mouse Build 38 (GCA_000001635.5)) was produced by the Mouse Genome Reference Consortium (http://genome.ucsc.edu/). Reads were normalized using DESeq and the normalized read counts were log-transformed and base-lined to the data set, resulting in normalized signal values. Differential gene expression of the normalized signal values between the control and experimental group was done using a moderated t-test, $P < 0.05$. The differentially expressed gene list was subsequently used for clustering and pathway analysis.

Statistical Analysis (NGS)

We used student's t-test to analyze the data. Statistical significance was evaluated by algorisms integral to the aforementioned software. P values of <0.05 were considered significant.

Lipid composition analysis

We followed the previously described method of lipid composition analysis (30). The colonic mucosal tissue extracts were subjected to acid hydrolysis/methanolysis to generate fatty acid methyl esters (FAMEs). FAMEs were separated from other lipids by TLC on Silica Gel 60 plates using a solvent system of 80:20 hexane/ether. FAMEs were quantified using an Agilent Technologies 6890N gas chromatograph with a flame ionization detector. We measured the following fatty acids: 1) Saturated Fatty Acids - myristic acid (14:0), pentadecanoic acid (15:0), palmitic acid (16:0), and stearic acid (18:0), 2) Monounsaturated

Fatty Acids - palmitoleic acid (16:1n-7) and oleic acid (18:1n-9), and 3) Polyunsaturated Fatty Acids (PUFA) - n-3 PUFA, α-linolenic acid (ALA, 18:3n-3), EPA (20:5n-3), DHA (22:6n-3), docosapentaenoic acid (DPA, 22:5n-3), n-6 PUFA, linoleic acid (18:2n-6), dihomo-γ-linolenic acid (DGLA, 20:3n-6), and arachidonic acid (20:4n-6). Fatty acids with a readout below detection levels were assigned the value of 0. We thank Lipid Analysis Core at Dean McGee Eye institute for fatty acid analysis.

Immunoblots, immunohistochemistry (IHC), and immunofluorescence

We used the following primary antibodies in 1–2 μg/ml: anti-CD36 (Santa Cruz Biotechnology, TX, sc-9154), anti-actin (Santa Cruz, sc-1616), anti-Numb (biorbyt, CA, orb6554), anti-JAG1 (Jagged1; Santa Cruz, SC-8303), anti-MSI1 (Musashi1; Santa Cruz, sc-98845), anti-CD24 (Santa Cruz, sc-11406), anti-CDKN1 p27 (Novus Biologicals, NB100-82093), and anti-γ-tubulin (Sigma, MO, T9026). Standard immunoblotting procedures were followed as described previously (19). Colonic mucosal tissues were extracted in extraction buffer with homogenizer, then boiled with SDS loading buffer for 5 minutes. Protein concentration was quantified using a protein assay dye reagent (Biorad, CA), and equalized. Immune complexes were detected with appropriate secondary antibodies conjugated with horseradish peroxidase (Sigma) and with chemiluminescence reagents (Thermo Scientific, MA). For statistical analysis, signals in blots were quantified with Image J software (http://rsb.info.nih.gov/ij/). Protein expressions were standardized with control (actin or tubulin) expression in the corresponding lane, and compared with unpaired t-test with Welch's correction with Graphpad Prizm 6 software. P values of <0.05 were considered significant.

Our IHC and immunofluorescence protocols were described in (25) in detail. For calculating percentage, three to seven slides from different animals were analyzed, and at least 400 cells per picture were counted.

FACS analysis

Mouse colons were dissociated for isolation of CD24, CD8a, and NK cells using a gentleMACS Dissociator and a MACSmixTM Tube Rotator according to manufacturer's instructions (Miltenyi Biotech, CA). The dissociated single cell suspensions from colons were labeled with the respective antibodies for CD24-Alexa Fluor-488, CD8a-APC, and NK cells (Nkp1.1-APC and Nkp46-PE), and active cells by IFN-γ-Alexa Fluor-488 staining, analyzed on a FACScalibur and data were analyzed by FlowJo software.

Results

Gene expression profiling in normal-looking colon tissues from Sgo1 and wild-type mice

To investigate transcriptomic changes in colonic tissues from Sgo1 haploinsufficient mice (hereafter, Sgo1 mice), we performed Next Generation Sequencing/RNAseq using the normal-looking part of colonic mucosal tissues of Sgo1 and control wild-type animals from a previous study (26), as the samples were well-characterized. At the endpoint, numbers in ACF and microscopic tumor were counted under microscope and determined comparable (26), thus cancer tissue contamination in the samples affecting the results was improbable.

The sample numbers met the requirements for statistical significance per Mead's resource equation (6 per group). Overall, the gene expression profiles showed a pattern of differences between the control and Sgo1 groups in the heat map (Figure 1). A principal components analysis indicated that the control and Sgo1 samples were grouping together.

Using the data set, we identified differentially expressed genes. There were total 349 hits with a 2-fold expression difference threshold, $P<0.05$ (217 upregulated genes, 132 downregulated genes; Examples in Table 1A). Significantly affected pathways (z-score >2) were identified, and indicated as Kyoto Encyclopedia of Genes and Genomes (KEGG) pathways (Table 1B left, upregulated pathways; Table 1B right, downregulated pathways).

We anticipated that DNA damage and/or growth regulatory pathways would appear among the most affected. However, the most affected upregulated genes were involved in biosynthesis of unsaturated fatty acids (z=4.47). The Notch signaling (z=4.47), insulin signaling (z=3.81), PPAR signaling (z=3.75), colorectal cancer-associated (z=3.64), and mismatch repair (z=3.47) pathways were also strongly affected (Table 1B). Thus, the regulation of metabolism and receptor-ligand-based growth were most affected. Activation of mismatch repair may be due to an increase in DNA damage.

The downregulated genes that were most impacted were involved in the allograft rejection (z=6.69), cyanoamino acid metabolism (z=6.61), graft-vs-host disease (z=6.54), and type I diabetes mellitus (z=6.20) pathways (Table 1B). These findings strongly suggest the impairment of or a modulation in immune responses in colonic tissues from Sgo1 mice.

Upregulations in lipid metabolism-related genes and CD36 as a potential marker for colonic CIN

Notably upregulated genes (e.g. CD36 (11.49-fold), Perilipin (6.21-fold), Adiponectin (5.73-fold); Figure 2A) involved in lipid metabolism. Sgo1 (reduced expression) and beta-actin (equal expression) are shown as controls (Figure 2A). CD36 is an integral membrane glycoprotein, a scavenger receptor, and is also known as fatty acid translocase (31, 32). Consistent with the findings from NGS/RNAseq, CD36 protein was shown to be upregulated in results from immunoblots and immunohistochemistry (Figure 2B). Detailed immunofluorescence analysis in AOM-untreated colon revealed the presence of CD36 in small infiltrating cells (Figure 2C, orange arrow) and a few distinctive colonocytes in Sgo1 colon tissues (Figure 2C, white arrow), but CD36 was not found in the extracellular matrix. In wild-type tissues, CD36 was detected primarily in small infiltrating cells. To test whether the CD36-positive colonocytes have CIN, we observed untreated colons from other transgenic model mice known to generate high CIN, namely spindle checkpoint BubR1$^{-/+}$ mice and *apc*$^{min/+}$ mice. Percentages of CD36-positive colonocytes in Sgo1, BubR1 and *apc* mice were significantly higher than that in wild type, providing a circumstantial evidence that CD36 is a marker of colon with high CIN.

Perilipin, also known as lipid droplet binding protein, coats and mobilizes lipid droplets in adipose tissue (33). Adiponectin functions as a protein hormone and modulates metabolic processes, including glucose regulation and fatty acid oxidation (34). Transgenic overexpression of perilipin in adipocytes protected the mice from obesity as a result of

feeding a high-fat diet (35). Overexpression of adiponectin in white adipocytes led to abrogation of adipocyte differentiation and weight loss in mice (36). However, the average body weight of the Sgo1 mice was comparable to that of controls (26).

From these results, we hypothesized that the colonic tissues of Sgo1 mice would show altered lipid composition. We analyzed the fatty acid composition in the mucosal tissues from AOM-treated and untreated wild-type (*N*=3) and Sgo1 colonic mucosal tissues (*N*=3) (Table 2). Notable differences in the lipid composition were found (marked in asterisks), implying that lipid metabolism is indeed affected in Sgo1 mice. In particular, DHA levels were consistently lower in Sgo1 mice both in AOM-treated and untreated conditions.

Upregulations in transcription factors

Consistent with gene expression changes in multiple pathways in Sgo1 mouse tissues, we found that several transcription factors are significantly upregulated in colonic tissues of Sgo1 mice. Among these were Tcf7 (2.73-fold), Foxa2 (2.10-fold), Foxq1 (2.14-fold), and Hox genes (Hoxa9 (2.97-fold). Hoxa13 (2.83-fold), Hoxa3 (2.14-fold)) which are involved in differentiation and in many cancers, including colon cancers (37).

Upregulation of Notch pathway-related genes and stem cell marker proteins

The NGS analysis detected upregulation in the Notch signaling pathway, which is highly relevant to colon cancer (38, 39). Activation of Notch signaling is involved in colonic cancer stem cell maintenance (40, 41). We investigated the amount and localization of selected colonic (normal) stem cell markers (Figure 3). Immunoblots showed an increase in the Notch pathway inhibitory regulator Numb, and in colonic stem cell markers JAG1 (Jagged-1) ($P<0.05$), while MSI1 (Musahi-1), and Lgr5 showed a tendency toward increase but the high variance resulted in non-significant P values. In contrast, levels of CD24, a cell adhesion protein involved in leukocyte migration to the colon (42) and a colonic cancer stem cell marker (43), decreased in Sgo1 mice ($P<0.05$).

We used immunohistochemistry to investigate the localizations of the stem cell markers. Among the markers tested, Numb and Jag1 showed most notable differences (Figure 3B, 3C). Jag1 normally localizes to the bottom of colonic crypts, corresponding with normal stem cells. However, in a small number of crypts in Sgo1 mice, Jag1 localized in areas up to the midsection of the crypts. Overall, stem cell marker analysis indicated misregulation of stem cell markers in Sgo1 mice.

Immune cell functions were compromised in colons of untreated Sgo1 mice

Next, with the pathway analysis suggesting a decrease in immune response, we tested functions of immune system components in colons of 11–12 months-old AOM-untreated wild type control (N=3) and Sgo1 (N=3) (Figure 4). CD24 expressions were measured among all immune cells. In wild type, 68.27 ± 4.819% were CD24-high expressing cells. In contrast, only 43.70 ± 4.330% of total CD24 expressing cells in Sgo1 were high expressors, and there were clear separation between CD24-high expressing cells and CD24-low expressing cells (Figure 4A), confirming immunoblots in Figure 3A. CD24-positive cells were infrequent in Sgo1 colon (Figure 4A). Next (Fig 4B), we monitored CD8 positive

cytotoxic T cells. 80.27 ± 8.877% of CD8+ cells recovered from wild type colons are Interferon-γ positive, but only 34.83 ± 2.975% were from Sgo1 ($P<0.05$), indicating a majority of CD8+ cytotoxic T-cells in Sgo1 were either not activated or incapable of producing Interferon-γ and exert cytotoxicity. Consistently, in wild type CD8 positive cells were also IFN-γ positive, but in Sgo1 they didn't always colocalize (Fig 4B). Next, NK cell functions were tested with two sorting markers Nkp46 (Fig 4C) and Nkp1.1 (Fig 4D). Similar to CD8+ cytotoxic T-cells, there was a significant decrease in Interferon-γ-expressing NK cells in Sgo1 (Fig 4C, 4D). Together, the FACS results indicated that a significant population of CD8+cytotoxic T cells and Nkp46+ or Nkp1.1+ NK cells in the colons of Sgo1 mice were either not activated or incapable of producing Interferon-γ, confirming prediction from NGS analysis that the immune cell functions were partly dysfunctional in Sgo1.

Discussion

Previously, we observed that transgenic mice that carry mutations causing systemic CIN developed colon cancers differently from controls (7, 26). We questioned the underlying cause of the altered carcinogenesis profiles in the CIN models. In this study, we identified several affected pathways in the colons of the AOM-treated CIN model $Sgo1^{-/+}$ mice. In the absence of histological carcinogenesis, CIN tissues activated or repressed multiple pathways, some of which were previously reported to be involved in colonic carcinogenesis. Also notably, the gene expression changes were not associated with a change in overall crypt structure (e.g. elongation of crypts observed in *apc* mice (44, 45)). Our results showed that some characteristics of cancer can be acquired with CIN prior to the development of histological abnormalities, dysplasia and cancer. At this stage, cells probably still maintain most anti-carcinogenic signaling pathways, such as cell death and senescence. This likelihood makes it an ideal stage in which to introduce preventive agents to intervene in carcinogenesis.

The fatty acid biosynthesis, Notch signaling, PPAR, and insulin signaling pathways were activated, while immune responses such as the allograft rejection and Graft-vs-host disease pathways were unexpectedly repressed in the NGS analysis. Consistently, our results showed that immune cell functions were indeed compromised in AOM-untreated Sgo1-CIN mice (Fig 4). Together, the modulations of the pathways may provide favorable microenvironment to early colonic carcinogenesis (a hypothetical model is presented in Figure 5).

A legitimate question is that whether the NGS results from AOM-treated mice are the same with those from untreated mice. For following reasons it seems likely; (i) our pilot small scale NGS in untreated mice did show similar pattern (data not shown), (ii) lipid compositions and CD36 expression showed differences between untreated control and Sgo1, and (iii) immune repression indicated in NGS with AOM-treated mice was confirmed in untreated Sgo1 (Figure 4). Expanding NGS approach to untreated mice and other conditions will shed light on effects of CIN *in vivo*.

Fatty acid biosynthesis

Colon cancer transcriptome analysis indicated that fatty acid metabolism is altered in cancer. The lipidome is shown to correlate with colon cancer (46). Fatty Acid Binding Protein 1 (FABP1) is usually among the most upregulated genes in the colon cancer transcriptome (28), potentially to meet altered requirements for energy metabolism and to adopt to cancer's hypoxic and acidic microenvironment. However, it was surprising for histologically normal-looking tissues to already exhibit modifications in fatty acid metabolism.

We observed changes in the lipid composition in Sgo1 mice (Table 2). Lipid metabolism and the associated lipid-based signaling modulation can influence colon carcinogenesis in different ways. For example, the COX-2 and arachidonic acid-mediated inflammatory pathways, and amounts of omega-3 EPA and DHA, are well-established to influence colonic carcinogenesis (47). We observed unexpected reduction of arachidonic acid in Sgo1 (that may work as anti-inflammatory), as well as a decrease in DHA (that may work as pro-inflammatory). Our results suggest that modulating the lipid metabolism with a pharmaceutical agent or through diet may be a valid strategy to influence CIN.

Notch signaling

The Notch signaling pathway plays an important role in embryogenesis and cellular homeostasis, differentiation, and apoptosis through "canonical" and "non-canonical" pathways, a ligand- or transcription-independent function (38, 39). The canonical Notch pathway includes at least four Notch receptors (Notch 1–4) and five Notch ligands: Delta-like 1, 3, and 4, and Jagged 1 and 2. Numb functions as an inhibitor of Notch signaling by degrading Notch. During neurogenesis, Notch signaling promotes proliferative signaling, and Numb-mediated Notch inhibition promotes neural differentiation. Activation of the Notch pathway may play an oncogenic role in colon and pancreatic cancers (38). Notch signaling has also been found to play a pivotal role in cancer stem cell development. A number of Notch signaling and cancer stem cell-targeting strategies have been proposed for colon cancer prevention and therapy (40, 41). We observed misregulations in stem cell markers in Sgo1 mice, and this is the first report for CIN itself affecting stem cell regulations. This finding will lead to investigations on underlying mechanisms. For example, since Sgo1 defect can cause multiple centrosomes, it is tempting to speculate that the defect may disturb spindle orientation in the colonic stem cells, which may serve as a mechanistic basis for maintaining asymmetric division of stem cell and stemness (48). High-resolution imaging analysis focusing on dividing stem cells in Sgo1 mice is warranted to test the speculation.

PPAR and insulin signaling

PPAR alpha, gamma, and beta/delta are nuclear transcription factors that form heterodimers with Retinoid X receptor. Numerous studies indicated that PPARs are involved in colon cancer, although the mode of involvement has proved to be complex (49). Insulin receptor signaling is involved in glucose uptake and storage, lipid synthesis, protein synthesis, and mitogenic responses. These pathways have been associated with colon cancer (28). Our study placed the involvement of the PPAR and insulin signaling at the onset of CIN, an unexpectedly early stage in colon cancer development.

Allograft rejection and graft-vs-host disease pathways

Current cancer chemoprevention strategies lean on anti-inflammatory reagents, and downregulation of immune responses with CIN was counterintuitive. Our results and the mechanism investigation may allow fine-tuning of immunomodulation approach.

Immunosurveillance is involved in suppressing tetraploid cells in the colon (50). A weakened immune system may provide a microenvironment that promotes the survival of aneuploid cells and carcinogenesis. This study, for the first time, provided evidence that CIN may be involved in immune system suppression. Further study will reveal the mechanisms by which Sgo1-CIN leads to potential immune suppression. Current hypotheses under investigation include: (i) CIN causes direct injury to immune cells, (ii) CIN mediates damage to colonocytes, leading to activation of an anergic response, and (iii) CIN mediates proteotoxicity, leading to suppression of pro-inflammatory factors, such as IL-1 and IFN-γ. Proteotoxicity and ER stress is a downstream event of CIN (9, 10) and is also reported to inhibit IL-1 and IFN-γ (51). Alternatively, (iv) altered expression of CD24 (Figure 3A, 4A) may have a negative effect on leukocyte recruitment in the Sgo1 colon. $CD24^{-/-}$ mice have fewer leukocytes in the colon than do wild-type mice (42). Further identifying the sequence of events connecting CIN and immune responses would lead to immuno-preventive/therapeutic agents for cells with CIN.

Possibility of CIN response conservation among species

This study uncovered many pathways that were not previously associated with CIN. Although unexpected, our results were at least partly consistent with findings using other model systems. In synthetic lethal screenings with a genetically tractable *Drosophila Melanogaster* model, a CIN-causing Mad2 mutant showed synthetic lethality with metabolism modulator genes (8). Taken together, these findings suggest that the cellular responses to CIN may be conserved among species, including insects.

Possibility of CIN-specific targeting through differentially expressed markers

For clinical translation, we aim to use our results to identify genes that indicate (i) that CIN can be used as a risk assessment marker or to distinguish CIN cells for targeting, and/or (ii) that CIN are involved in early stage carcinogenesis, and can thus be inhibited in order to prevent cancer. We identified CD36 by applying additional criteria: a cell surface protein, and the knockdown or inhibition of which is not known to cause disease (Figure 2). A gene product that meets all of these criteria may be an ideal target for vaccination and other antibody-based targeting approaches. The validity of CD36 for the targeting approach is being tested, yet the use of the transcriptome would be beneficial for identifying potential targets that could be used in combination with secondary screening.

In summary, we used a transgenic CIN model to identify several pathways that were not previously connected to CIN. These results and further validation would provide numerous unexpected targets for intervention in colonic carcinogenesis for chemo- and dietary-prevention purposes.

Supplementary Material

Refer to Web version on PubMed Central for supplementary material.

Acknowledgments

Funding statements

This work was supported by grants from the U.S. National Institutes of Health to C.V. Rao (NCI R01CA094962), W. Dai (RO1CA090658), and H.Y. Yamada (NCI RO3CA162538); also supported by a Chris4Life colon cancer foundation pilot study grant to H.Y. Yamada. Additionally, this project (or publication) was supported by the National Center for Research Resources and the National Institute of General Medical Sciences of the National Institutes of Health through Grant Number 8P20GM103447 [Oklahoma's IDeA Network for Biomedical Research Excellence (OK-INBRE)] to the OUHSC Microgen core facility. The funders had no role in study design, data collection and analysis, decision to publish, or preparation of the manuscript.

References

1. Bakhoum SF, Silkworth WT, Nardi IK, Nicholson JM, Compton D, Cimini D. The mitotic origin of chromosomal instability. Curr Biol. 2014; 24:R148–R149. [PubMed: 24556433]
2. Carter SL, Eklund AC, Kohane IS, Harris LN, Szallasi Z. A signature of chromosomal instability inferred from gene expression profiles predicts clinical outcome in multiple human cancers. Nat Genet. 2006; 38:1043–1048. [PubMed: 16921376]
3. Sotillo R, Schvartzman JM, Socci ND, Benezra R. Mad2-induced chromosome instability leads to lung tumour relapse after oncogene withdrawal. Nature. 2010; 464(7287):436–440. [PubMed: 20173739]
4. Dunican DS, McWilliam P, Tighe O, Parle-McDermott A, Croke DT. Gene expression differences between the microsatellite instability (MIN) and chromosomal instability (CIN) phenotypes in colorectal cancer revealed by high-density cDNA array hybridization. Oncogene. 2002; 21:3253–3257. [PubMed: 12082642]
5. American Cancer Society, statistics for 2015 (as of 3/15/2015). http://www.cancer.org/cancer/colonandrectumcancer/detailedguide/colorectal-cancer-key-statistics
6. Wood LD, Parsons DW, Jones S, Lin J, Sjöblom T, Leary RJ, et al. The genomic landscapes of human breast and colorectal cancers. Science. 2007; 318:1108–1113. [PubMed: 17932254]
7. Rao CV, Yamada HY. Genomic instability and colon carcinogenesis: from the perspective of genes. Front Oncol. 2013; 3:130. [PubMed: 23734346]
8. Shaukat Z, Liu D, Choo A, Hussain R, O'Keefe L, Richards R, et al. Chromosomal instability causes sensitivity to metabolic stress. Oncogene. 2015; 34(31):4044–4055. [PubMed: 25347746]
9. Oromendia AB, Dodgson SE, Amon A. Aneuploidy causes proteotoxic stress in yeast. Genes Dev. 2012; 26(24):2696–2708. [PubMed: 23222101]
10. Williams BR, Prabhu VR, Hunter KE, Glazier CM, Whittaker CA, Housman DE, et al. Aneuploidy affects proliferation and spontaneous immortalization in mammalian cells. Science. 2008; 322(5902):703–709. [PubMed: 18974345]
11. Schvartzman JM, Sotillo R, Benezra R. Mitotic chromosomal instability and cancer: mouse modelling of the human disease. Nat Rev Cancer. 2010; 10(2):102–115. [PubMed: 20094045]
12. Rao CV, Yamada HY, Yao Y, Dai W. Enhanced genomic instabilities caused by deregulated microtubule dynamics and chromosome segregation: a perspective from genetic studies in mice. Carcinogenesis. 2009; 30(9):1469–1474. [PubMed: 19372138]
13. Foijer F, Draviam VM, Sorger PK. Studying chromosome instability in the mouse. Biochim Biophys Acta. 2008; 1786(1):73–82. [PubMed: 18706976]
14. Ricke RM, van Ree JH, van Deursen JM. Whole chromosome instability and cancer: a complex relationship. Trends Genet. 2008; 24(9):457–466. [PubMed: 18675487]
15. Duijf PH, Benezra R. The cancer biology of whole-chromosome instability. Oncogene. 2013; 32(40):4727–4736. [PubMed: 23318433]

16. Weaver BA, Silk AD, Montagna C, Verdier-Pinard P, Cleveland DW. Aneuploidy acts both oncogenically and as a tumor suppressor. Cancer Cell. 2007; 11(1):25–36. [PubMed: 17189716]
17. Iwaizumi M, Shinmura K, Mori H, Yamada H, Suzuki M, Kitayama Y, et al. Human Sgo1 downregulation leads to chromosomal instability in colorectal cancer. Gut. 2009; 58(2):249–260. [PubMed: 18635744]
18. Kahyo T, Iwaizumi M, Shinmura K, Matsuura S, Nakamura T, Watanabe Y, et al. A novel tumor-derived SGOL1 variant causes abnormal mitosis and unstable chromatid cohesion. Oncogene. 2011; 30(44):4453–4463. [PubMed: 21532624]
19. Yamada HY, Yao Y, Wang X, Zhang Y, Huang Y, Dai W, et al. Haploinsufficiency of SGO1 results in deregulated centrosome dynamics, enhanced chromosomal instability and colon tumorigenesis. Cell Cycle. 2012; 11(3):479–488. [PubMed: 22262168]
20. Yun C, Cho H, Kim SJ, Lee JH, Park SY, Chan GK, et al. Mitotic aberration coupled with centrosome amplification is induced by hepatitis B virus X oncoprotein via the Ras-mitogen-activated protein/extracellular signal-regulated kinase-mitogen-activated protein pathway. Mol Cancer Res. 2004; 2:159–169. [PubMed: 15037655]
21. Wen Y, Golubkov VS, Strongin AY, Jiang W, Reed JC. Interaction of hepatitis B viral oncoprotein with cellular target HBXIP dysregulates centrosome dynamics and mitotic spindle formation. J Biol Chem. 2008; 283:2793–2803. [PubMed: 18032378]
22. Kim S, Park SY, Yong H, Famulski JK, Chae S, Lee JH, et al. HBV X protein targets hBubR1, which induces dysregulation of the mitotic checkpoint. Oncogene. 2008; 27:3457–3464. [PubMed: 18193091]
23. Wang LH, Huang W, Lai MD, Su IJ. Aberrant cyclin A expression and centrosome overduplication induced by hepatitis B virus pre-S2 mutants and its implication in hepatocarcinogenesis. Carcinogenesis. 2012; 33:466–472. [PubMed: 22159224]
24. Baek KH, Park HY, Kang CM, Kim SJ, Jeong SJ, Hong EK, et al. Overexpression of hepatitis C virus NS5A protein induces chromosome instability via mitotic cell cycle dysregulation. J Mol Biol. 2006; 359:22–34. [PubMed: 16616934]
25. Yamada HY, Zhang Y, Reddy A, Mohammed A, Lightfoot S, Dai W, et al. Tumor-promoting/progressing role of additional chromosome instability in hepatic carcinogenesis in Sgo1 (Shugoshin 1) haploinsufficient mice. Carcinogenesis. 2015 Mar 4. pii: bgv011. PMID: 25740822.
26. Rao CV, Sanghera S, Zhang Y, Biddick L, Reddy A, Lightfoot S, et al. Antagonizing pathways leading to differential dynamics in colon carcinogenesis in Shugoshin1 (Sgo1)-haploinsufficient chromosome instability model. Mol Carcinog. 2015 Mar 14. PMID: 25773652.
27. Gao C, Furge K, Koeman J, Dykema K, Su Y, Cutler ML, et al. Chromosome instability, chromosome transcriptome, and clonal evolution of tumor cell populations. Proc Natl Acad Sci U S A. 2007; 104(21):8995–9000. [PubMed: 17517657]
28. Habermann JK, Paulsen U, Roblick UJ, Upender MB, McShane LM, Korn EL, et al. Stage-specific alterations of the genome, transcriptome, and proteome during colorectal carcinogenesis. Genes Chromosomes Cancer. 2007; 46(1):10–26. [PubMed: 17044061]
29. Stevens JB, Horne SD, Abdallah BY, Ye CJ, Heng HH. Chromosomal instability and transcriptome dynamics in cancer. Cancer Metastasis Rev. 2013; 32(3–4):391–402. [PubMed: 23595307]
30. Mohammed A, Janakiram NB, Brewer M, Duff A, Lightfoot S, Brush RS, et al. Endogenous n-3 polyunsaturated fatty acids delay progression of pancreatic ductal adenocarcinoma in Fat-1-p48(Cre/+)-LSL-Kras(G12D/+) mice. Neoplasia. 2012; 14(12):1249–1259. [PubMed: 23308056]
31. Pepino MY, Kuda O, Samovski D, Abumrad NA. Structure-function of CD36 and importance of fatty acid signal transduction in fat metabolism. Annu Rev Nutr. 2014; 34:281–303. [PubMed: 24850384]
32. Abumrad NA, Davidson NO. Role of the gut in lipid homeostasis. Physiol Rev. 2012; 92(3):1061–1085. [PubMed: 22811425]
33. Bickel PE, Tansey JT, Welte MA. PAT proteins, an ancient family of lipid droplet proteins that regulate cellular lipid stores. Biochim Biophys Acta. 2009; 1791(6):419–440. [PubMed: 19375517]

34. Barb D, Williams CJ, Neuwirth AK, Mantzoros CS. Adiponectin in relation to malignancies: a review of existing basic research and clinical evidence. Am J Clin Nutr. 2007; 86(3):s858–s866. [PubMed: 18265479]
35. Miyoshi H, Souza SC, Endo M, Sawada T, Perfield JW 2nd, Shimizu C, et al. Perilipin overexpression in mice protects against diet-induced obesity. J Lipid Res. 2010; 51(5):975–982. [PubMed: 19797618]
36. Bauche IB, El Mkadem SA, Pottier AM, Senou M, Many MC, Rezsohazy R, et al. Overexpression of adiponectin targeted to adipose tissue in transgenic mice: impaired adipocyte differentiation. Endocrinology. 2007; 148(4):1539–1549. [PubMed: 17204560]
37. Bhatlekar S, Fields JZ, Boman BM. HOX genes and their role in the development of human cancers. J Mol Med (Berl). 2014; 92(8):811–823. [PubMed: 24996520]
38. Ranganathan P, Weaver KL, Capobianco AJ. Notch signalling in solid tumours: a little bit of everything but not all the time. Nat Rev Cancer. 2011; 11:338–351. [PubMed: 21508972]
39. Andersen P, Uosaki H, Shenje LT, Kwon C. Non-canonical Notch signaling: emerging role and mechanism. Trends Cell Biol. 2012; 22:257–265. [PubMed: 22397947]
40. Sikandar SS, Pate KT, Anderson S, Dizon D, Edwards RA, Waterman ML, et al. NOTCH signaling is required for formation and self-renewal of tumor-initiating cells and for repression of secretory cell differentiation in colon cancer. Cancer Res. 2010; 70(4):1469–1478. [PubMed: 20145124]
41. Kemper K, Grandela C, Medema JP. Molecular identification and targeting of colorectal cancer stem cells. Oncotarget. 2010; 1(6):387–395. [PubMed: 21311095]
42. Bretz NP, Salnikov AV, Doberstein K, Garbi N, Kloess V, Joumaa S, et al. Lack of CD24 expression in mice reduces the number of leukocytes in the colon. Immunol Lett. 2014; 161(1): 140–148. [PubMed: 24956310]
43. Naumov I, Zilberberg A, Shapira S, Avivi D, Kazanov D, Rosin-Arbesfeld R, et al. CD24 knockout prevents colorectal cancer in chemically induced colon carcinogenesis and in APC(Min)/CD24 double knockout transgenic mice. Int J Cancer. 2014; 135(5):1048–1059. [PubMed: 24500912]
44. Sansom OJ, Reed KR, Hayes AJ, Ireland H, Brinkmann H, Newton IP, et al. Loss of Apc in vivo immediately perturbs Wnt signaling, differentiation, and migration. Genes Dev. 2004; 18(12): 1385–1390. [PubMed: 15198980]
45. Dow LE, O'Rourke KP, Simon J, Tschaharganeh DF, van Es JH, Clevers H, et al. Apc Restoration Promotes Cellular Differentiation and Reestablishes Crypt Homeostasis in Colorectal Cancer. Cell. 2015; 161(7):1539–1552. [PubMed: 26091037]
46. Hodge A, Williamson EJ, Bassett JK, MacInnis RJ, Giles GG, English DR. Dietary and biomarker estimates of fatty acids and risk of colorectal cancer. Int J Cancer. 2015; 137(5):1224–1234. [PubMed: 25683336]
47. Janakiram NB, Rao CV. The role of inflammation in colon cancer. Adv Exp Med Biol. 2014; 816:25–52. [PubMed: 24818718]
48. Inaba M, Yamashita YM. Asymmetric stem cell division: precision for robustness. Cell Stem Cell. 2012; 11(4):461–469. [PubMed: 23040475]
49. Zuo X, Xu M, Yu J, Wu Y, Moussalli MJ, Manyam GC, et al. Potentiation of colon cancer susceptibility in mice by colonic epithelial PPAR-δ/β overexpression. J Natl Cancer Inst. 2014; 106(4) dju052.
50. Boilève A, Senovilla L, Vitale I, Lissa D, Martins I, Métivier D, et al. Immunosurveillance against tetraploidization-induced colon tumorigenesis. Cell Cycle. 2013; 12(3):473–479. [PubMed: 23324343]
51. Weber SM, Chambers KT, Bensch KG, Scarim AL, Corbett JA. PPARgamma ligands induce ER stress in pancreatic beta-cells: ER stress activation results in attenuation of cytokine signaling. Am J Physiol Endocrinol Metab. 2004; 287(6):E1171–E1177. [PubMed: 15315910]
52. Vries RG, Huch M, Clevers H. Stem cells and cancer of the stomach and intestine. Mol Oncol. 2010; 4(5):373–384. [PubMed: 20598659]

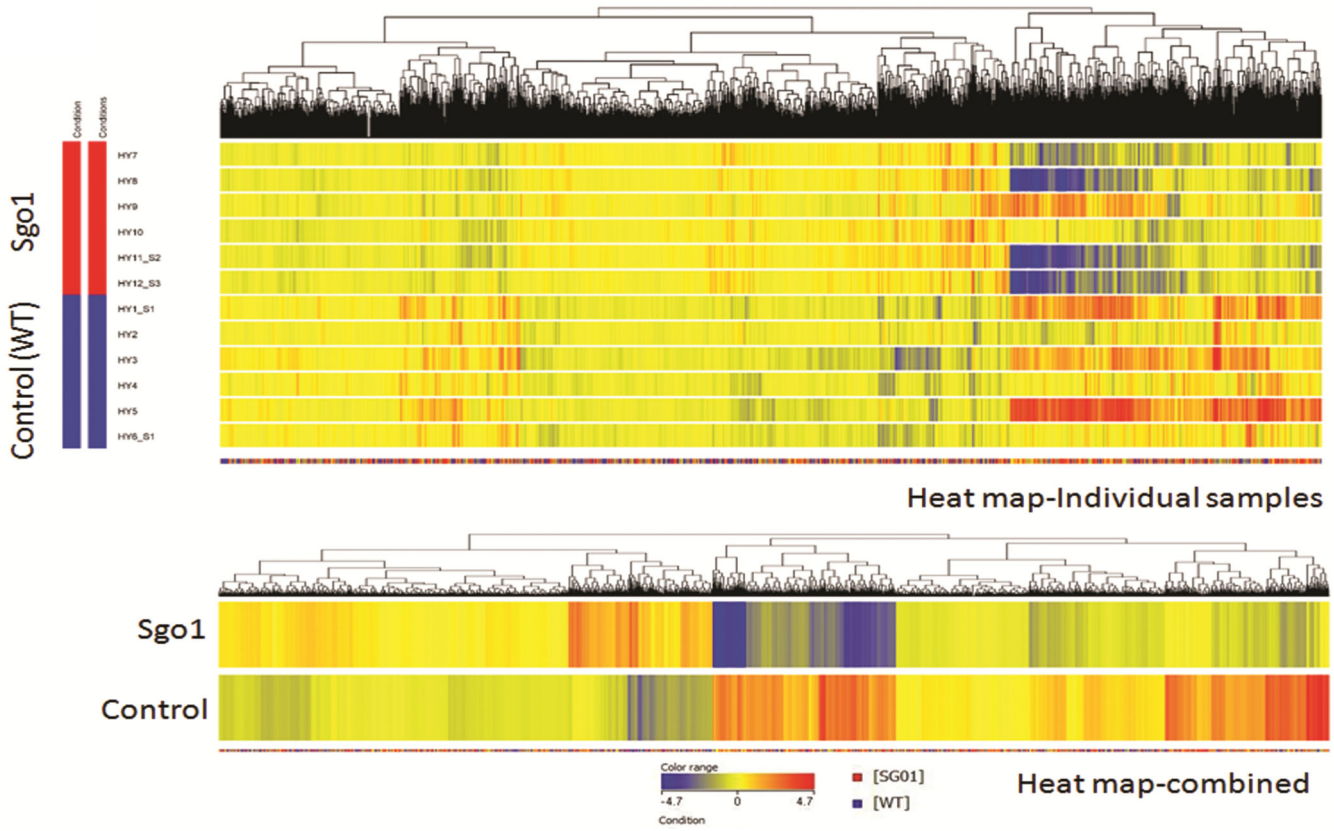

Figure 1. Consistent differences in gene expression profiles between Sgo1 and control wild-type mice

The heat map indicated consistent differences in gene expression profiles between two groups. A supervised Hierarchical clustering algorithm using normalized intensity values was done. Similarity measure: Euclidean; Linkage rules: Wards. Each row represents the normalized expression values for individual mice in the control or Sgo1 group. The columns represent how the normalized values cluster according to expression for all samples. The colors represent the range of gene expression. Blue would indicate a reduced expression value and red an increased expression value. The deeper color is a higher expression values whether reduced or increased.

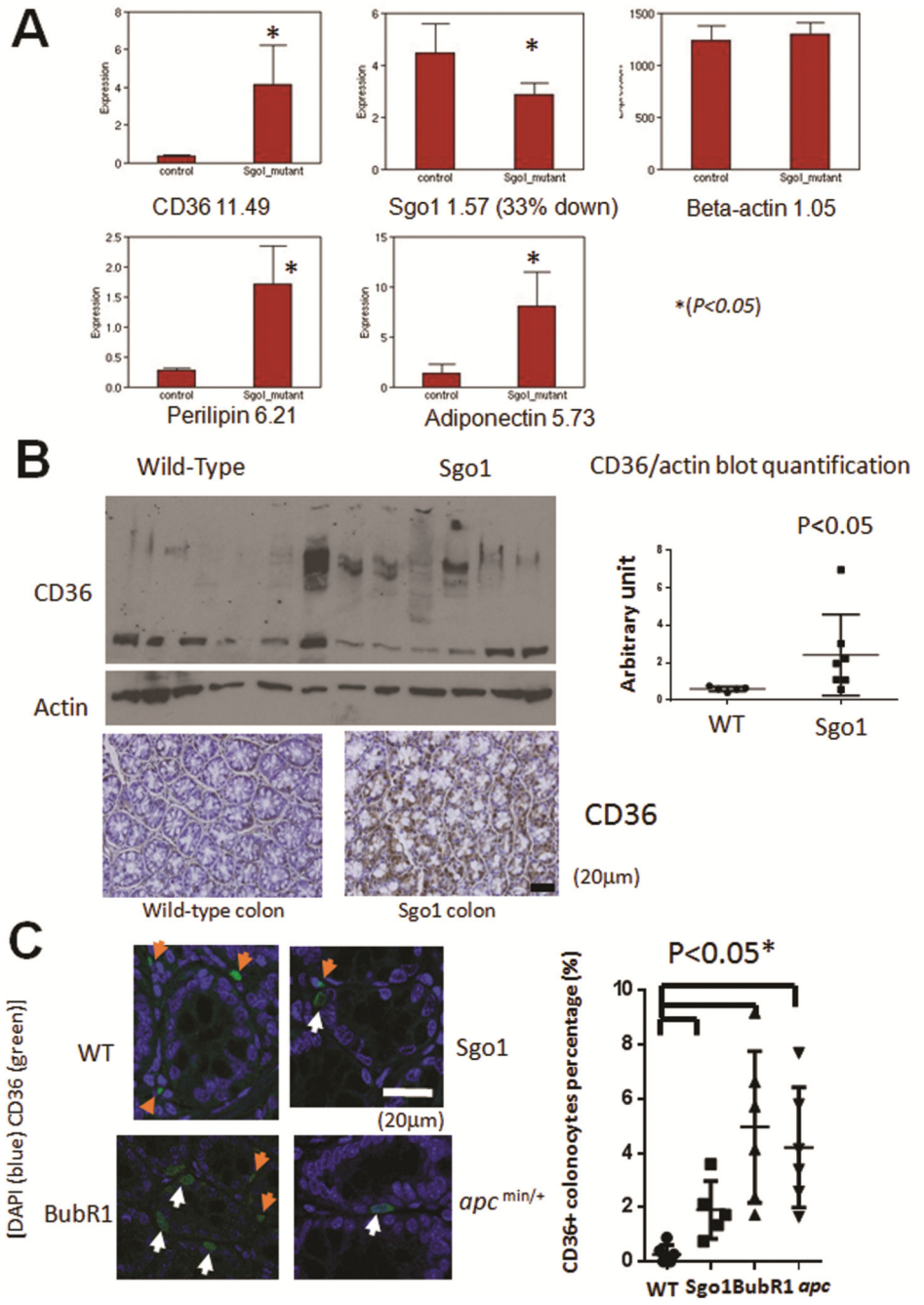

Figure 2. Genes involved in lipid metabolism are among the most affected in Sgo1 mice

(A) 11.49-fold change in CD36. Perilipin and Adiponectin are also shown. Asterisk indicates $p<0.05$. Expression unit is relative and arbitrary. Sgo1 mRNA showed a 33% decrease in Sgo1 mice, consistent with haploinsufficiency and indicative of accuracy in NGS standardization. NGS expression estimate in beta-actin was equal in control and in Sgo1 mice, also indicating accuracy in NGS standardization. (B) Consistent with RNAseq, CD36 protein was over-expressed in Sgo1 mice; in immunoblots (top left panels - CD36 is a glycoprotein and the glycosylated form appears as smear; actin is the loading control) and in

immunohistochemistry (bottom panels, brown signal). (C) Immunofluorescence indicated that CD36 (green) expression was limited in infiltrating small cells (orange arrow) in wild type. In Sgo1 mice and other CIN-generating mice BubR1 and *apc*, CD36 was observed in colonocytes (white arrow) in addition to infiltrating cells (see text). The percentages of CD36-positive colonocytes were significantly higher in the transgenic models with high CIN (i.e. Sgo1, BubR1 and *apc*) than in control, suggesting that CD36 expression in colonocytes is associated with high CIN.

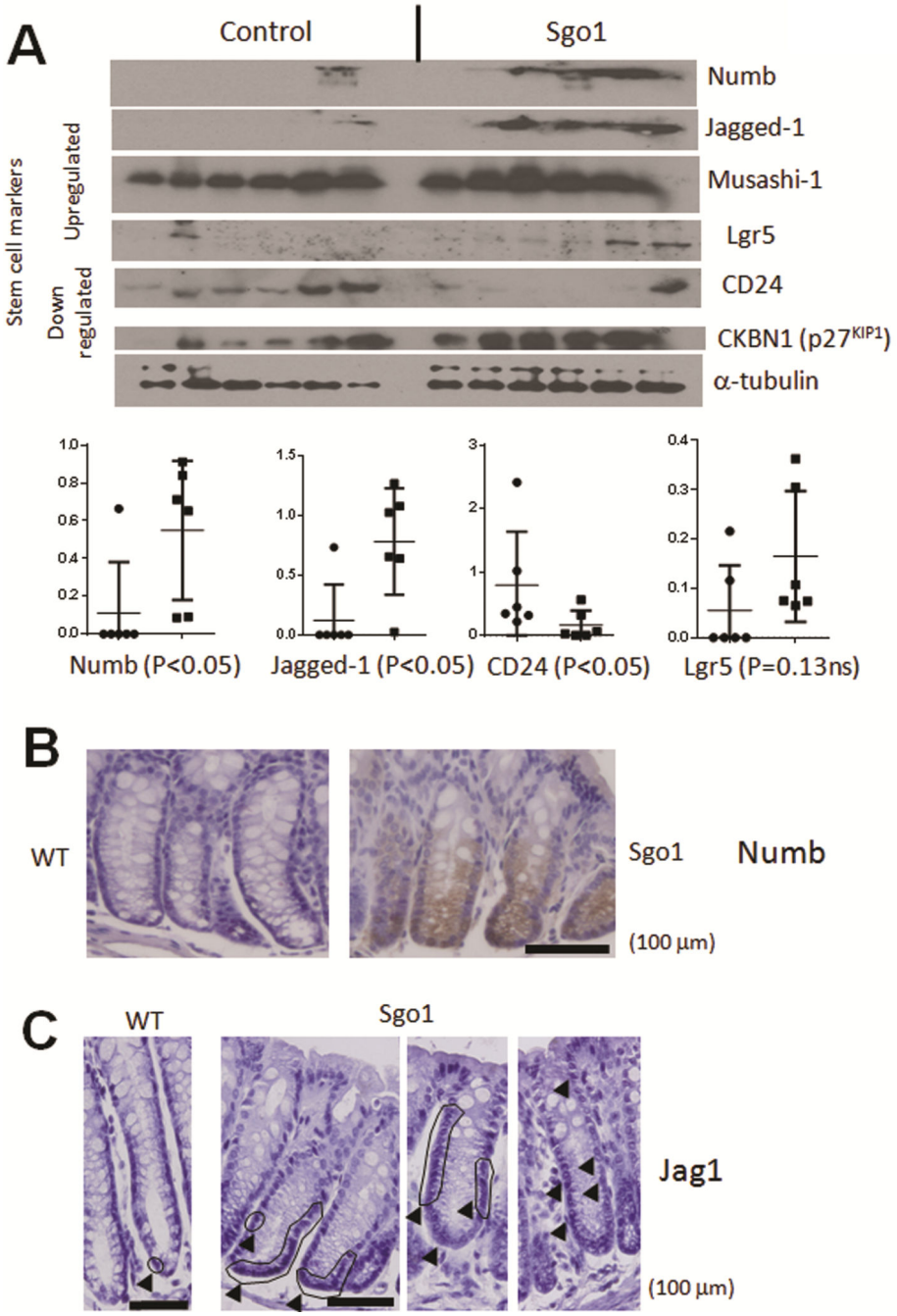

Figure 3. Stem cell markers are misregulated in Sgo1 mice

(A) Numb (negative regulator of Notch pathway), colonic normal and cancer stem cell markers Jagged-1 (Jag1), Musashi-1 (Msi1), and Lgr5 were upregulated, while another stem cell marker, CD24, was downregulated. Increased CKBN1 ($p27^{KIP1}$) suggests that growth inhibition is also activated through the senescent pathway, as previously noted in the AOM-treated mice (19, 26). The left six lanes are control wild-type, while the right six lanes are Sgo1. Each sample was from a different animal. Numb, Jag1 and CD24 met statistical significance with immunoblots. (B) IHC for Numb. Numb protein localized in the bottom

half of Sgo1 crypts. As in the immunoblot analysis, upregulation was evident. (C) Jagged-1 localized in a small number of stem cells in the bottom of wild-type colonic crypts and in most Sgo1 crypts (circled or arrow). However, Jagged-1 was mislocalized in a few Sgo1 crypts.

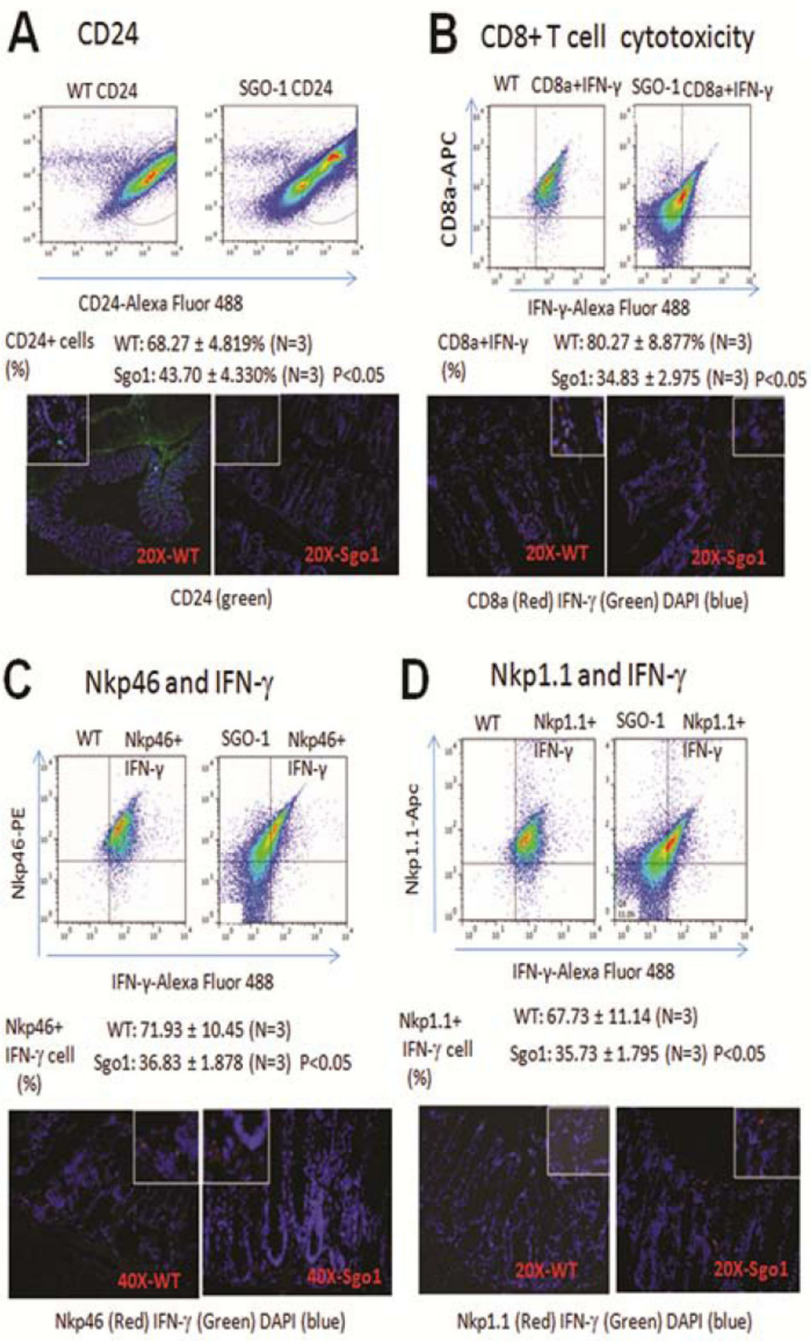

Figure 4. Immune cells were dysfunctional in the colons of untreated Sgo1 mice

(A) A significant population of colon-derived cells in Sgo1 showed a decrease in CD24+ expression (top panels). In wild type, CD24 (green) is normally observed in colon-infiltrating leukocytes. CD24+ cells were decreased in Sgo1 colon (bottom panels). (B) (top panels) CD8+ Cytotoxic T cells were sorted by FACS, and expression of Interferon-γ was monitored. Percentages of CD8+IFN-γ+ among all colonic immune cells was significantly decreased in Sgo1 ($P<0.05$). (bottom panels) In wild type, CD8+ cells (red) were producing IFN-γ+ (green), but in Sgo1, not all cells co-expressed CD8 and IFN-γ. (C) NK cells were

sorted with Nkp46 marker, and expression of Interferon-γ was monitored. Percentages of Nkp46+IFN-γ+ was significantly decreased in Sgo1 (upper panels). IFN-γ-expressing NK cells were decreased in Sgo1 (bottom panel). (D) NK cells were sorted with Nkp1.1 marker, and expression of Interferon-γ was monitored. The same results as (C) were observed in Nkp46 and Nkp1.1 NK cell marker.

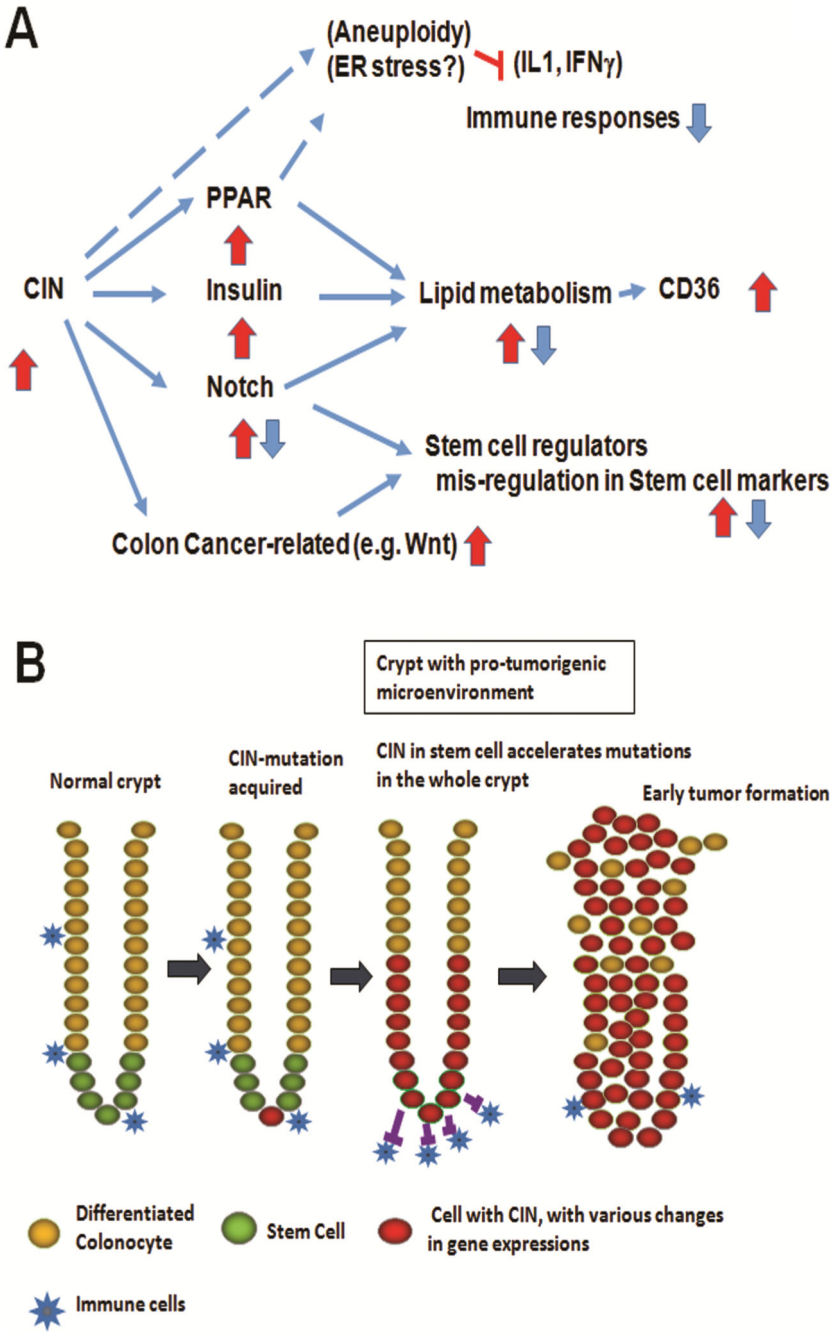

Figure 5. Hypothetical models for CIN in early carcinogenesis in colonic crypts

(A) CIN is a triggering event to activate many receptor-mediated signaling pathways including PPAR, Insulin, Notch and Wnt. PPAR, Insulin and Notch pathways regulate lipid metabolism, leading to a modification in lipid composition. Notch and Wnt pathways regulate stem cell markers directly or indirectly, leading to alterations in stem cell markers. CIN and resulting aneuploidy and/or ER stress affect Interleukin or Interferon, eventually repressing immune cells.

(B) Colonic crypt is generated from a limited number of stem cells (ref 52). When a mutation that causes CIN is introduced into the (normal) stem cell in a colonic crypt, the mutation will affect all cells that form the crypt. If such a mutation occurs in a non-stem cell, the effect is unlikely to be permanent, as crypt cells will be shed in the turnover process. However, once stem cells acquire a CIN-causing mutation (as in Sgo1 mice), the CIN will accelerate accumulation of further mutations, driving the whole crypt toward carcinogenesis. As the transcriptome suggests, crypt cells with CIN would develop changes in metabolic and proliferative profiles while suppressing immune surveillance for aneuploid cells. That would create a microenvironment favorable to further transformation. Then eventually CIN results in colon cancer. Many pathways in the colon cancer transcriptome are shared with the (Sgo1-) CIN transcriptome.

Table 1

Normal-looking colonic mucosal tissues from Sgo1 mice differentially expressed genes involved in the lipid metabolism, Notch signaling, insulin signaling, and peroxisome proliferator-activated receptor (PPAR) pathways.

(A) Up- or Down-regulated Genes				
Upregulated Genes (Top30, Examples)				
No.	**Ratio**	**p-value**	**Identifier**	
1	11.49	0.00214	Cd36	CD36 antigen, mRNA (cDNA cloneMGC:6068 IMAGE:3481681)
2	8.06	0.00257	S3–12	Premature mRNA for mKIAA1881 protein
3	6.50	0.01704	H2-K1	Histocompatibility 2, K1, K region, mRNA (cDNA clone MGC:7052 IMAGE:3156482)
4	6.21	0.00796	Pln	Perilipin (Pln), transcript variant 2, mRNA
5	6.18	0.01109	Aoc3	Amine oxidase, copper containing 3 (Aoc3), mRNA
6	5.73	0.01198	Adipoq	Adiponectin, C1Q and collagen domain containing, mRNA (cDNA clone MGC;41360 IMAG
7	5.66	0.02980	Cfd	Complement factor D (adipsin) (Cfd), mRNA
8	5.59	0.01011	Abcd2	ATP-containing cassette, sub-family D (ALD), member2, mRNA (cDNA clone 291101
9	5.21	0.01057	Nnat	Neuronatin, mRNA (cDNA clone MGC:46898 IMAGE:4981517
10	5.19	0.00017	Hmcn1	Hemicentin 1(Hmcn1), mRNA
11	4.69	0.00464	Rps18	Ribosomal protein S18 (Rps18), mRNA
12	4.49	0.00023	Sh3bgr	Putative SH3BGR protein (SH3BGR gene)
13	4.38	0.03216	Car3	Carbonic anhydrase 3, mRNA (cDNA clone MGC:18583 IMAGE:4195712)
14	4.33	0.00150	Bex4	Brain express gene 4, mRNA (cDNA clone MGC:116687 IMAGE:30677421)
15	4.28	0.00013	Camk2b	Calcium/calmodulin-dependant protein kinase II, beta (Camk2b), mRNA
16	4.21	0.02696	Npr3	Natriuretic peptide receptor 3 (Npr3), transcript variant 1, mRNA
17	4.17	0.00038	Slc2a4	Solute carrier family 2 (facilitated glucose transporter), member 4, mRNA (cDNA
18	4.08	0.00095	Eda2r	Ectodysplasin A2 isoform receptor, mRNA (cDNA clone MGC:124099 IMAGE:40045945)
19	4.01	0.00095	Btn1a1	Butyrophilin, sub family 1, member A1, mRNA (cDNA clone MGC:25305 IMAGE:3582574)
20	3.94	0.04636	Sncg	Synuclein, gamma, mRNA (cDNA clone MGC:41140 IMAGE:1448798)
21	3.86	0.00084	Gpsm3	G-protein signaling modulator 3 (AGS3-like, C.elegans) (Gpsm3), mRNA
22	3.80	0.02348	Chodl	Chondrolectin (Chodl), mRNA
23	3.69	0.02301	100503531	hypothetical LOC100503531
24	3.68	0.00218	Npy1r	Neuropeptide Y receptor Y1 (Npy1r), mRNA
25	3.59	0.03620	Capn6	Calpain 6 (Capn6), mRNA

(A) Up- or Down-regulated Genes				
Upregulated Genes (Top30, Examples)				
No.	**Ratio**	**p-value**	**Identifier**	
26	3.46	0.00396	Trf	Transferrin (Trf), mRNA
27	3.43	0.01236	Ccdc80	Coiled-coil domain containing 80 (Ccdc80), mRNA
28	3.41	4.35e-05	Prkar2b	Protein kinase, cAMP dependent regulatory, type II beta (Prkar2b), mRNA
29	3.40	0.00122	Fzd4	Frizzled homolog 4 (Drosophila), mRNA (cDNA clone MGC:18403 IMAGE:4238940)
30	3.39	0.00322	EG624219	Predicted gene, EG624219, mRNA (cDNA clone IMAGE:5050186)

Downregulated Genes (Top20, examples)				
No.	**Ratio**	**p-value**	**Identifier**	**Gene Name**
1	11.40	0.00486	Reg3b	Regenerating islet-derived 3 beta, mRNA (cDNA clone MGC:41159 IMAGE:3471932)
2	9.15	0.00794	Reg3g	Regenerating islet-derived 3 gamma (Reg3g), mRNA
3	7.86	0.00239	668474	Immunoglobulin heavy variable V1–7
4	6.19	0.00150	Ighv6–6	Anti-HLA class II antibody gamma F3,3 heavy chain variable region
5	5.64	0.01287	380805	Immunoglobulin heavy variable V10–1
6	5.23	0.00018	100503705	Hypothetical protein LOC100503705
7	5.13	0.01307	Ighv1–19	Clone H226 monoclonal autoantibody heavy chain variable region
8	4.81	0.01438	Igfbp6	Insulin-like growth factor binding protein 6, mRNA (cDNA clone MGC:14073 IMAGE:4
9	4.54	0.03170	667914	Immunoglobulin kappa variable 3–12
10	4.53	0.01055	Lrrn4	Neuronal leucine rich repeat 4
11	4.37	0.00197	Oxct2a	TISP 10 mRNA, complete cds, increased in spermiogenesis
12	4.03	0.00326	Gnmt	Glycine N-methyltransferase, mRNA (cDNA clone MGC:13738 IMAGE:4210236)
13	3.97	0.01887	ENSMUSG00000074178	PREDICTED: Mus musculus predicted gene, ENSMUSG00000074178 (ENSMUSG00000074178),
14	3.94	0.02564	238418	Immunoglobulin heavy variable V14–3
15	3.88	0.00080	Snord118	Clone MBI-34 C/D box snoRNA, partial sequence
16	3.79	0.00134	380823	Immunoglobulin heavy variable V1–64
17	3.79	0.01584	EG232801	Predicted gene, EG232801 (EG232801), mRNA
18	3.71	0.03978	780825	Immunoglobulin heavy variable V9–3
19	3.69	0.04144	404743	Immunoglobulin lambda variable 3
20	3.52	0.02633	692169	Immunoglobulin kappa chain variable 32 (V32)

(B) Up- or Down-regulated Pathways	
Upregulated Pathways (Z-score>2.0)	
Pathways	**Z-score**
Biosynthesis of unsaturated fatty acids	4.47
Notch signaling pathway	4.47
Insulin signaling pathway	3.81
PPAR signaling pathway	3.75
Colorectal cancer	3.64
Progesterone-mediated oocyte maturation	3.48
Mismatch repair	3.47
Beta-alanine metabolism	3.36
Nitrogen metabolism	3.36
Homologous recombination	2.98
Type II diabetes mellitus	2.66
Endometrial cancer	2.52
Gastric acid secretion	2.51
DNA replication	2.41
Basal cell carcinoma	2.39
Melanogenesis	2.39
Base excision repair	2.29
Fatty acid biosynthesis	2.29
ECM-receptor interaction	2.10
Purine metabolism	2.06
Vitamin B-6 metabolism	2.06
Aminoacyl –tRNA biosynthesis	2.03

Downregulated Pathways (Z-score>2.0)	
Pathways	**Z-score**
Allograft rejection	6.69
Cyanoamino acid metabolism	6.61
Graft-versus-host disease	6.54
Type- I diabetes mellitus	6.20
Autoimmune thyroid disease	5.75
Antigen processing and presentation	5.23
Taurine and hypotaurine metabolism	5.04
Natural killer cell mediated cytotoxicity	4.86
Viral myocarditis	4.82
Glutathione metabolism	4.07
Pantothenate and CoA biosynthesis	4.04
Drug metabolism – other enzymes	3.86
Axon guidance	3.68
endocytosis	3.66

Downregulated Pathways (Z-score>2.0)	
Pathways	**Z-score**
Cell adhesion molecules (CAMs)	3.43
Selenoamino acid metabolism	3.16
Biosynthesis of unsaturated fatty acids	3.01
Phagosome	3.01
Phototransduction	2.75
Melanogenesis	2.72
Osteoclast differentiation	2.42
Intestinal immune network for IgA production	2.17
Hepatitis C	2.14
Vasopressin-regulated water reabsorption	2.13
Linoleic acid metabolism	2.07
MAPK signaling pathway	2.06

(A) Examples of the most upregulated 30 and downregulated 20 genes. P-values were calculated with modified Student's t-test (*N*=6 for both Sgo1 and control groups). For standardization, "total mapped genes" were used. Full list of 349 up- or down-regulated genes is provided as Supplementary Figure 1. (B) Upregulated and Downregulated pathways in Sgo1 mice. Z-scores higher than 2 are listed. Notably, many pathways are involved in immune responses.

Table 2

Fatty acid analysis

Lipid composition analysis in colonic mucosal tissues from control and Sgo1 mice (AOM-treated and untreated) indicated altered lipid compositions in Sgo1 mice.

Fatty acids	Wild Type AOM	Sgo1 AOM	Wild Type Saline	Sgo1 Saline
14:0 (myristic)	1.21±0.28	1.22±0.23	1.91±0.85	1.79±0.74
16:0 (palmitic)	23.66±3.57	22.81±1.17	25.66±5.84	27.36±6.79
16:1	3.57±0.37	3.87±0.52	6.52±2.41	5.40±2.27
18:0 (stearic)	7.30±3.64	8.04±1.13	9.78±4.97	8.75±5.19
18:1 (oleic)	25.87±5.99	25.97±1.29	29.01±2.41	29.84±3.90
18:2n6 (linoleic)	27.53±5.64	26.08±0.92	13.72±2.64	16.39±1.75*
18:3n3 (ALA)	1.15±0.34	1.08±0.13	0.54±0.21	0.59±0.14
20:0	0.23±0.12	0.25±0.05	0.31±0.20	0.25±0.21
20:1	0.80±0.24	0.77±0.24	0.65±0.35	0.53±0.27
20:4n3	0.07±0.03	0.11±0.63	0.19±0.13	0.13±0.13
20:5n3 (EPA)	0.47±0.25	0.35±0.03	1.20±0.86	1.14±1.12
20:2n6	0.37±0.15	1.70±0.28*	0.25±0.14	0.29±0.20
20:3n6 (DGLA)	1.21±0.61	3.99±0.14*	2.51±1.76	1.52±1.41
20:4n6 (arachidonic)	4.33±3.58	0.25±0.05*	4.50±3.27	3.29±2.93
22:0	0.11±0.16	0.19±0.08	0.33±0.22	0.29±0.26
22:1	0.10±0.03	0.30±0.04*	0.19±0.13	0.17±0.16
22:4n6	0.22±0.11	0.09±0.01*	0.25±0.18	0.19±0.16
22:5n6	0.07±0.03	0.43±0.06*	0.12±0.08	0.08±0.06
22:5n3 (DPA)	0.31±0.11	1.58±0.10*	0.37±0.22	0.34±0.29
22:6n3 (DHA)	1.13±0.57	0.17±0.03*	1.65±1.08	1.32±1.13*
24:0	0.12±0.08	0.17±0.03	0.20±0.13	0.21±0.17
24:1	0.13±0.09	0.12±0.01	0.13±0.08	0.12±0.09

(Mean±SD)

Lipids in the control (*N*=3) and Sgo1 (*N*=3) tissues were solvent-extracted and quantified with gas chromatography. Numbers represent percentages (mean-/+SD).

* Asterisks indicate notable and significant differences. Notably, DHA is reduced in Sgo1 colon both in AOM-treated and untreated conditions.